Phys. Status Solidi C **9**, No. 7, 1651–1654 (2012) / **DOI** 10.1002/pssc.201200024

physica status solidi c
www.pss-c.com
current topics in solid state physics

Fabrication and applications of orientation-patterned gallium arsenide for mid-infrared generation

A. Grisard[*,1], F. Gutty[1], E. Lallier[1], B. Gérard[2], and J. Jimenez[3]

[1] Thales Research & Technology France, 1 av. Augustin Fresnel, 91767 Palaiseau Cedex, France
[2] III-V Lab, 1 av. Augustin Fresnel, 91767 Palaiseau Cedex, France
[3] GdS Optronlab, Fisica Materia Condensada, Universidad de Valladolid, 47011 Valladolid, Spain

Received 28 March 2012, accepted 30 March 2012
Published online 30 May 2012

Keywords GaAs, HVPE, mid infrared, optical losses

[*] Corresponding author: e-mail arnaud.grisard@thalesgroup.com

Nonlinear optical materials play a key role in the development of coherent sources of radiation, by frequency conversion of light from other light sources, e.g. diode, solid-state, and fiber lasers, into spectral ranges where few lasers exist or perform poorly. Based on the principle of the quasi-phase matching, the design and fabrication of orientation-patterned Gallium Arsenide crystals (OP-GaAs) has recently led to demonstrations of second harmonic generation, optical parametric generation, amplification and oscillation from 1 to 12 µm. The most efficient fabrication route for these crystals relies on the use of the near-equilibrium growth process HVPE (Hydride Vapour Phase Epitaxy), by orientation-selective regrowth on OP-GaAs template wafers with a thickness suited to bulk nonlinear optics. This work deals with recent characterizations based on optical experiments and cathodoluminescence measurements, targeting the identification of the main defects, their spatial distribution, and their relation to the optical propagation losses. Latest improvements of the HVPE growth step have enabled to reach an unprecedented level of losses, below 0.016 cm^{-1}, and a large range of available QPM periods and thickness of structures.

© 2012 WILEY-VCH Verlag GmbH & Co. KGaA, Weinheim

1 General Mid–IR laser sources are necessary for diverse applications. Nonlinear optical materials are very useful for the development of coherent sources of radiation as they allow the frequency conversion of mature diode, solid-state and fiber lasers light into spectral ranges where few lasers exist or perform poorly. An attractive approach to perform those sources consists of non linear optical conversion by the quasi phase matching (QPM) method using GaAs [1,2], which is a semiconductor with a large non linear optical coefficient (≅100 pm/V), a high transparency in the 1-16 µm spectral range, a high laser damage threshold, and a mature epitaxy technology. Because GaAs is an isotropic material, non linear optical conversion cannot be done by periodical poling, as for ferroelectrics. However, such conversion can be achieved by stacking GaAs plates with alternate crystallographic orientation, [001]/[00-1]. This constitutes a grating structure where the non linear optical coefficient is periodically inverted [3]. The period of these structures can be predefined to produce laser sources with wavelengths ranging from 1 to 12 µm, which proves a very versatile technology suited to an increasing number of applications that demand mid-IR light sources. The design and epitaxial fabrication of orientation-patterned GaAs (OP-GaAs) wafers has thus lately led to demonstrations of second harmonic generation, optical parametric generation, amplification and oscillation in the spectral window of 1 to 12 µm [4].

The most efficient fabrication route for these crystal structures relies on the use of the near-equilibrium growth process by Hydride Vapour Phase Epitaxy (HVPE), yielding high quality orientation-selective regrowth on specifically prepared OP-GaAs template wafers with a thickness suited to bulk nonlinear optical conversion. We present herein a description of the growth procedure, as well as the characterization of these crystals using spectrally resolved cathodoluminescence (SRCL) [5,6], targeting the identification of the main defects, their spatial distribution and their potential relation to the optical propagation losses.

© 2012 WILEY-VCH Verlag GmbH & Co. KGaA, Weinheim

The latest improvements of the HVPE growth step have enabled to reach an unprecedented level of optical losses, below 0.016 cm^{-1}, and a large range of available QPM periods and thickness of structures, which opened this technique to a large set of applications. One can contemplate the implementation of OP-GaAs crystals in various configurations, suitable for applications such as frequency metrology by cascaded IR upconversion [7], local gas sensing with a broadly tunable single-frequency mid-infrared source based on difference frequency generation [8], mid-infrared remote sensing by optical parametric amplification of a distributed feedback quantum cascade laser in OP-GaAs [9], or directed infrared countermeasures thanks to a compact fiber laser-pumped optical parametric oscillator [10].

2 OP-GaAs crystal growth The need for thick structures requires fast epitaxial growth procedures with excellent selectivity. The method of choice for achieving fast growth rates is the HVPE. The epitaxial growth on orientation-patterned semiconductor crystals suitable for QPM conversion requires templates with modulated crystalline orientation, constituting the seeds for the epitaxial regrowth. In a compound III-V semiconductor with zincblende structure, such as GaAs, the reverse orientation consists of the exchange of the atoms between the two sublattices (Ga and As), which is equivalent to a reversal of the III-V bond stacking. The templates can be fabricated by photolithography, on crystals with the two crystal orientations, [001] and [00-1], formed by the wafer bonding method. Two GaAs wafers are bonded with opposite crystal axis orientation. Next, the [00-1] side is lapped until only a thin [00-1] layer remains on the [001] wafer; then, the domain periods and duty cycles are defined by photolithography, and the patterned template is etched to reveal the orientation-patterned gratings [11].

The second stage of the fabrication consists of the regrowth on the OP-GaAs template to obtain the thick OP-GaAs crystal required for bulk optical pumping. In order to optimize the QPM the crystallographic orientations must be preserved all along the growth process, keeping the duty cycle of the domains equal to the one defined on the template, usually 1:1. Atmospheric pressure HVPE [12,13] provides efficient growth of high quality GaAs layers with hundreds of µm thickness at high growth rates. The HVPE growth is mainly limited by the adsorption of the gaseous molecules onto the surface, decomposition of the ad-species and desorption processes. HVPE growth is perfectly orientation-selective as it depends on the intrinsic growth anisotropy of the crystal, which can be controlled by the growth temperature and the precursor gas composition [14]. The typical HVPE growth rate stands close to 30 µm/h for GaAs in an atmospheric HVPE reactor due to the high decomposition rate of the growth precursors. However, the high growth rate results in parasitic nucleation on the reactor walls, which depletes the nutrients, changes the effective gas flow rates, and decreases the crystal growth rate. To maintain a constant vapour composition, growth interruptions had to be made every few hours in earlier experiments for cleaning the reactor. Recent improvements enabled us to carry out much longer growth cycles, up to 30 hours, without cleaning. This in practice led to an increase in the final OP-GaAs layer thickness from typically 0.5 mm up to more than 1 mm.

The OP-GaAs crystals were studied by CL in order to determine the presence of defects, as well as the properties of the walls separating adjacent [001] and [00-1] domains. CL measurements were carried out with a mono-CL system from Gatan UK, attached to a field emission scanning electron microscope (FESEM) Carl-Zeiss Leo 1530. The CL signal was spectrally resolved, and spectrum images were obtained in selected regions of interest. The measurements were carried out at 80 K.

3 Results and discussion The studies of these structures target the understanding of the main defects and impurities introduced during the crystal growth, which can be deleterious because of their contribution to the QPM efficiency and the optical propagation losses.

The nonlinear conversion efficiency can be reduced by several kinds of deviations of real OP-GaAs layers from the ideal periodic structure for a given interaction: domain annihilation by preferential growth of neighbour domains, deflection of domain walls, modification of the duty cycle, etc. Figure 1 shows a panchromatic CL image with some defects concerning the grating periodicity.

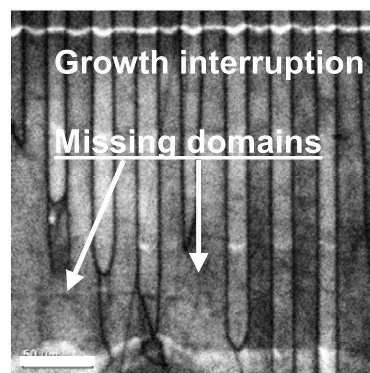

Figure 1 Panchromatic CL image showing a growth interruption and some missing domains (the bar is 50 µm). The growth direction is from top to bottom.

An important cause of optical propagation losses stems from the presence of crystal defects, both point defects and impurities and extended defects. In particular, the domain walls can be considered as extended defects in addition to dislocations, precipitates, etc. The contribution of these defects to optical losses can be related to, optical absorption, light scattering, and back reflections associated with parasitic refractive index changes. The optical absorption in the near infrared spectral range is governed by the impurities and point defects. This mostly concerns the absorption of

© 2012 WILEY-VCH Verlag GmbH & Co. KGaA, Weinheim

the pumping light often chosen around 2 μm wavelength, to avoid two photon absorption phenomena. The presence of free carriers, consequence of unintentional doping with residual impurities is responsible for the intraband absorption in the long wavelength ranges [15]. Thus, the identification of the main defects in thick OP-GaAs crystals is crucial to improve the growth methods of these crystals. The panchromatic CL images reveal a marked contrast between [001] and [00-1] domains, Fig. 2.

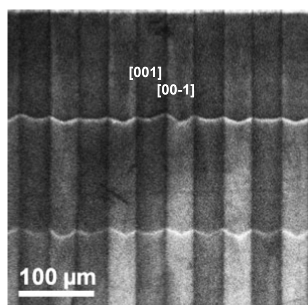

Figure 2 Panchromatic CL image showing the contrast between the two domain orientations, and the growth interruptions.

In general, the luminescence efficiency of the [00-1] domains is higher than the one of the [001] domains, which is the consequence of a higher concentration of deep levels in [001] domains with respect to [00-1] domains. The main deep levels in GaAs are related to excess As [16]. This suggests a higher incorporation rate of As in [001] than in [00-1] domains, which is governed by the faceting of the growth fronts in the two domains. The CL intensity along the growth direction, does not show a systematic evolution with the distance to the seed, which means that the parasitic nucleation reduces the growth rate but does not significantly alter the rate of incorporation of non-radiative recombination centers, mainly responsible for the CL contrast. The growth interruptions, necessary to clean the reactor and to restore the growth rate, generally appear as bright luminescence planes in the CL images, see Figs. 1, and 2; however, the CL decays very quickly once the growth is restarted, reaching the luminescence level measured before the interruption after a few microns regrowth.

On the other hand, the CL images reveal a dark contrast for the domain walls, which points to non-radiative recombination activity. An antiphase boundary is ideally formed of antibonds As-As and Ga-Ga that are active non-radiative recombination centers. Along the domain walls the luminescence intensity decreases by a factor of 2 with respect to the body of the [001] domains, and by a factor of 3 with respect to the body of the [00-1] domains. This is the consequence of the non-radiative recombination activity of the walls [17]; however, this quenching is very small with respect to the regions of the domains beyond a minority carrier diffusion length from the walls. This suggests that the antibonds, both As-As and Ga-Ga on the (0-11) crystallographic plane of the wall, are mostly inhibited, and therefore, have a much lower non-radiative recombination activity than expected for an antiphase domain boundary formed by antibonds. Epitaxial layers with antiphase domains, undergo a luminescence quenching of over 4 orders of magnitude with respect to layers without antiphase domains. Such a quenching was drastically reduced when doping with Si, for which only a factor of ten decrease was reported [17]. This inhibition of the non-radiative recombination was related to Si sitting at the antibonds. In our samples, the doping level is residual, therefore, one can assume that point defects are formed at the domain boundaries inhibiting the antibonds, with the corresponding reduction of the non-radiative recombination rate.
The spectrally resolved CL analysis reveals the distribution of the different luminescence bands, and therefore of the main defects present in these crystals. Typical CL spectra are shown in Fig. 3.

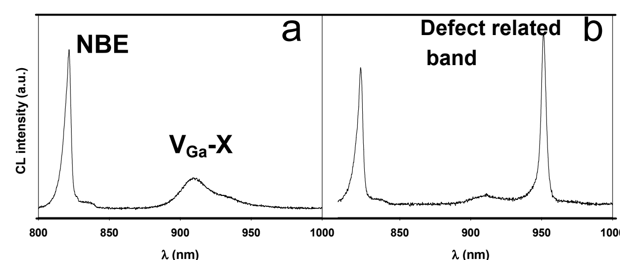

Figure 3 CL spectra, a) domain body, b) selected zones of the domain wall.

These spectra are typical of undoped GaAs, slightly As rich. The CL spectra show three main luminescence bands. The near band edge (NBE) spectral region, with a symmetric band peaking at 822 nm, is associated with a bound excitonic transition, and an asymmetric component in the high energy tail corresponding to band to band recombination. An additional weak band is observed in the low energy side of the excitonic band, which is associated with an e-A^o transition. A broad band is observed at 910 nm; this band, typical of undoped GaAs, is associated with gallium vacancy complexes, V_{Ga}-X, and is distributed all over the GaAs OP-crystal. The overall presence of this band suggests that the HVPE layers grow under As rich conditions. A band peaking at 950 nm is also observed along the domain walls, Fig. 3.

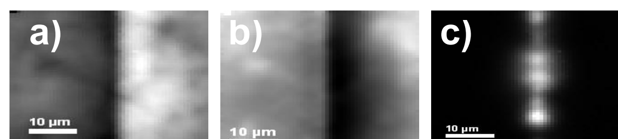

Figure 4 Monochromatic CL images, a) NBE, b) relative intensity of the 910 nm band (V_{Ga-X} related), c) monochromatic image at 950 nm (defect related band) showing inhomogeneous distribution along the domain wall.

© 2012 WILEY-VCH Verlag GmbH & Co. KGaA, Weinheim

Monochromatic images of the main emissions are shown in Fig. 4. The distribution of the different luminescence bands reveals that the domain walls are decorated by defects.

Transmission electron microscopy of the domain walls does not evidence discontinuity between the planes of the two domain orientations, Fig. 5; therefore, the main defects at the domain walls are point defects or impurities, in agreement with the CL data.

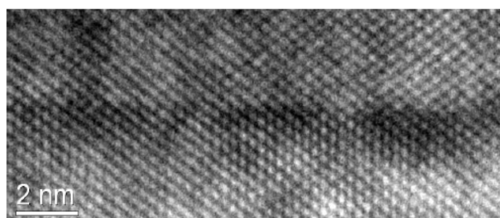

Figure 5 TEM view of domain wall, where one observes the continuity between the crystallographic plans between the two domain orientations.

The decoration of the walls by those defects induces strain that can be monitored by the shift of the excitonic peak at the domain walls, Fig. 6. This strain modifies the refractive index, which contributes to back reflections at the domain walls. Optical propagation losses as low as 0.016 cm^{-1} have been measured. Strained-induced Fresnel back reflections are much lower, even taking into account long samples with small QPM periods, i.e. with a large number of domain walls. Nevertheless, these tiny back-reflections can have detrimental consequences on counter-directional optical mode coupling when implementing OP-GaAs samples in ring cavities [18].

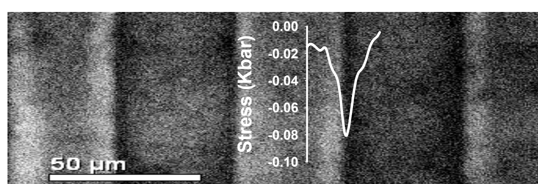

Figure 6 CL image with stress profile across the domain wall as deduced from the NBE shift

4 Conclusion Optimized OP-GaAs crystals with a low defect concentration and a well-defined grating period and duty cycle over the targeted geometrical characteristics, constitute very versatile mid-IR laser sources. The control of residual impurities and their incorporation enables a strong decrease in propagation losses. Loss values as low as 0.016 cm^{-1} have been obtained. The microscopic characterizations are essential to establish relations between the growth parameters and the microscopic defects, and between those defects and the propagation losses. This opens preferred routes towards future quality control tools and procedures for improvements in process yield.

Acknowledgements This work has been supported by the European Commission through FP6 project VILLAGE (Versatile Infrared Laser source for Low-cost Analysis of Gas Emissions) and FP7 project MIRSURG (Mid-Infrared Solid-State Laser Systems for Minimally Invasive Surgery). J. J. was also funded by Spanish Government (MAT-2010-20441-C02).

References

[1] O. Levi, T. J. Pinguet, T. Skauli, L. A. Eyres, K. R. Parameswaran, J. S. Harris, Jr., M. M. Fejer, T. J. Kulp, S. E. Bisson, B. Gerard, E. Lallier, and L. Becouarn, Opt. Lett. **27**, 2091 (2002).
[2] C. Lynch, D. F. Bliss, T. Zens, A. Lin, J. S. Harris, P. S. Kuo, and M. M. Fejer, J. Cryst. Growth **310**, 5241 (2008).
[3] E. Lallier, M. Brevignon, and J. Lehoux, Opt. Lett. **23**, 1511 (1998).
[4] K. L.Vodopyanov, O. Levi, P. S. Kuo, T. J. Pinguet, J. S. Harris, M. M. Fejer, B. Gerard, L. Becouarn, and E. Lallier, Opt. Lett. **29**, 1912 (2004).
[5] D. Faye, A. Grisard, E. Lallier, B. Gérard, M. Avella, and J. Jimenez, Appl. Phys. Lett. **93**, 151115 (2008).
[6] O. Martínez, M. Avella, V. Hortelano, J. Jiménez, C. Lynch, and D. Bliss, J. Electron. Mater. **39**, 805 (2010).
[7] L. Becouarn, E. Lallier, M. Brévignon, and J. Lehoux, Opt. Lett. **23**, 1508 (1998).
[8] S. Vasilyev, S. Schiller, A. Nevsky, A. Grisard, D. Faye, E. Lallier, Z. Zhang, A. J. Boyland, J. K. Sahu, M. Ibsen, and W. A. Clarkson, Opt. Lett. **33**, 1413 (2008).
[9] G. Bloom, A. Grisard, E. Lallier, C. Larat, M. Carras, and X. Marcadet, Opt. Lett. **35**, 505 (2010).
[10] A. Grisard, F. Gutty, E. Lallier, and B. Gerard, in: Proc. SPIE 783606 (2010).
[11] E. Lallier, D. Faye, A. Grisard, and B. Gerard, in: Proc. SPIE **5990**, 599001 (2005).
[12] J. B. Theeten, L Hollan, and R. Cadoret, Crystal Growth and Materials (North-Holland, 1977).
[13] E. Gil, J. Napierala, A. Pimpinelli, and R. Cadoret, J. Cryst. Growth **258**, 14 (2003).
[14] E. Gil, J. Napierala, D. Castelluci, A. Pimpinelli, R. Cadoret, and B. Gérard, J. Cryst. Growth **222**, 482 (2001).
[15] W. G. Spitzer and J. M. Whelan, Phys. Rev. **114**, 59 (1959).
[16] J. C. Bourgoin, H. Hammadi, M. Stellmacher, J. Nagle, B. Grandidier, D. Stievenard, J. P. Nys, C. Delerue, and M. Lannoo, Physica B **273/274**, 725 (1999).
[17] G. Brammertz, Y. Mols, S. Degroote, V. Motsnyi, M. Leys, G. Borghs, and M. Caymax, J. Appl. Phys. **99**, 093514 (2006).
[18] S. Vasilyev, H.-E. Gollnick, A. Nevsky, A. Grisard, E. Lallier, B. Gérard, J. Jimenez, and S. Schiller, Appl. Phys. B **100**, 737(2010).

© 2012 WILEY-VCH Verlag GmbH & Co. KGaA, Weinheim